

UDC 621.362.192

DOI: 10.15587/1729-4061.2021.240259

This paper reports a comparative analysis of the thermal regime control means while minimizing a set of basic parameters in various combinations with the indicators of reliability and dynamics of the functioning of a single-stage thermoelectric cooler. The connection has been established between the optimal relative operating current corresponding to the minimum of the set on the relative temperature difference and heat sink capacity of the radiator. The results of calculating the main parameters, reliability indicators, time of entering the stationary mode of operation for various current modes of operation at a fixed temperature difference, thermal load at different geometry of the branches of thermoelements are given. A comparative analysis of the main parameters, indicators of the reliability and operational dynamics of a single-stage cooler under various characteristic current modes of operation has been carried out. Minimizing the set of basic parameters in conjunction with the reliability indicators and operational dynamics of the cooling thermoelement provides a decrease in the refrigeration coefficient up to 40 % compared to the maximum cooling capacity mode, as well as the optimal heat sink capacity of the radiator, the amount of energy expended, the time of entering the stationary mode, the relative intensity of failures. The analysis of the influence of the temperature difference at a predefined thermal load on the relative operating current, the time it takes for the cooler to enter the stationary thermal regime, the heat sink capacity of the radiator, the relative intensity of failures has been performed. The devised method of optimal control over the thermal regime of a single-stage thermoelectric cooler based on minimizing the set of basic parameters makes it possible to search for and select compromise solutions, taking into consideration the weight of each of the limiting factors

Keywords: thermoelectric cooler, set of basic indicators, geometry of thermoelements, dynamic characteristics, reliability indicators

COMPARATIVE ANALYSIS OF MEANS TO CONTROL THE THERMAL REGIME OF A COOLING THERMOELEMENT WHILE MINIMIZING THE SET OF BASIC PARAMETERS

Vladimir Zaykov

PhD, Head of Sector
Research Institute «STORM»
Tereshkovoi str., 27, Odessa, Ukraine, 65076

Vladimir Mescheryakov

Doctor of Technical Sciences, Professor,
Head of Department
Department of Informatics

Odessa State Environmental University
Lvivska str., 15, Odessa, Ukraine, 65016

Yurii Zhuravlov

Corresponding author

PhD, Associate Professor

Department of Technology of Materials and Ship Repair
National University «Odessa Maritime Academy»

Didrikhsona str., 8, Odessa, Ukraine, 65029

E-mail: ivanovich1zh@gmail.com

Received date 17.08.2021

Accepted date 07.10.2121

Published date 29.10.2021

How to Cite: Zaykov, V., Mescheryakov, V., Zhuravlov, Y. (2021). Comparative analysis of means to control the thermal regime of a cooling thermoelement while minimizing the set of basic parameters. *Eastern-European Journal of Enterprise Technologies*, 5 (8 (113)), 38–50. doi: <https://doi.org/10.15587/1729-4061.2021.240259>

1. Introduction

Strict requirements for the weight and size characteristics and failure rates of heat-loaded onboard equipment for ensuring the thermal regimes of heat-loaded electronic equipment make the use of thermoelectric coolers alternative-free. The inclusion of a thermoelectric cooler in the negative feedback circuit of the control system requires an increase in the dynamic characteristics of the cooler, which fundamentally contradicts the reliability indicators. The relevance of scientific problems is due to the need to find such a current mode of the thermoelectric cooler, which contributes to finding a compromise between interrelated dynamic characteristics and reliability indicators. The practical significance of the results of such studies is to minimize the weight and size indicators and energy consumption of onboard equipment.

2. Literature review and problem statement

Paper [1] reports the conditions for the functioning of heat-loaded elements of electronic equipment and the means of ensuring their thermal regimes. However, the issues of improving the reliability of thermoelectric systems for ensuring thermal regimes have not been highlighted, although this parameter is decisive under the pulse-periodic mode for heat-loaded elements [2]. The influence of the load on the reliability indicators of the operating range of temperature differences and operating currents is described in [3] but the issues of the impact of the design parameters of the cooler remained unresolved. The connection of the energy interaction of the heat-releasing object with the current modes of the thermoelectric cooler is considered in work [4]. The influence of structural parameters on the reliability indicators of the thermoelectric cooler in harsh operating conditions

required studies aimed at improving operational reliability [5]. At the same time, the cited studies are limited to the static modes of operation of thermoelectric coolers although it is known that the rate of change in the temperature field adversely affects the reliability of the contact connection of the thermoelement with the electrode [6]. The dynamic characteristics of thermoelectric coolers were not given sufficient attention because according to these features, they are significantly superior to air and compression systems for ensuring thermal regimes [7]. Active systems for ensuring thermal regimes involve the inclusion of a thermoelectric cooler in the feedback circuit, which significantly increases the importance of the dynamic characteristics of the cooler [8]. The relationship of dynamic characteristics with reliability indicators is a fundamental problem [9], so further research is aimed at studying the influence of energy indicators and structural parameters. Changes in design parameters for the purpose of more effective removal of heat flow [10] and search for ways to increase operational reliability are considered. However, control issues related to the complex influence of the current modes of operation of the thermoelectric cooler, structural parameters in the operating temperature range remained unsolved. At the same time, the expansion of the scope of use of thermoelectric coolers expands the requirements for their control [11–13]. The choice of a set of interrelated parameters for controlling the thermoelectric cooler is an important task, resolving which could solve the problem of controlling the thermoelectric system for ensuring the thermal regimes of heat-loaded elements. The set of parameters should provide a compromise between the required dynamic characteristics, permissible reliability indicators of the thermoelectric cooler.

3. The aim and objectives of the study

The aim of this work is to identify the analytical connection of the set of basic parameters with the optimal thermal regime of a single-stage thermoelectric cooler. This will make it possible to minimize the weight and size characteristics of onboard systems for ensuring thermal regimes of heat-loaded electronic equipment.

To accomplish the aim, the following tasks have been set:

- to devise a model of a thermoelectric cooler in relation to a set of basic parameters;
- to analyze the dynamic characteristics and reliability indicators for the main current modes of thermoelectric coolers.

4. The study materials and methods

To build and analyze a mathematical model of the thermoelectric cooling device, we applied methods of thermophysical modeling of dynamic systems for ensuring thermal regimes of electronic equipment. The construction of the model is based on the law of conservation of energy; simplifications assume the homogeneity of the material of thermoelements and the identity of their geometric and thermophysical characteristics; the limitations are to neglect the distortions of the thermal field at the boundaries of removable electrodes [14]. Procedures of model calculations whose correctness is confirmed by the results of experimental studies when performing research and experimental design work are given in [14]. The connection of the dy-

amic characteristics of the thermoelectric cooler with the geometry and material of thermoelements, the structural technological features of the cooler, the energy performance indicators in the range of operating temperatures and loads is presented in [15].

5. The results of studying means to control the thermal mode of cooling thermoelement

5.1. Thermoelectric cooler model

Among the main parameters of the thermoelectric cooler (TEC), providing a predefined thermal mode of operation, are the structural, energy, operational, and dynamic ones. In particular, the number of thermoelements n , the value of the operating current I , the relative failure rate λ/λ_0 , the probability of trouble-free operation P , the time to enter the stationary mode of operation τ , the heat sink capacity of the radiator αF . This determines the set of interrelated basic parameters that affect the thermal mode of TEC operation. In the rational design of the TEC regime, one should strive to reduce $n, I, \lambda, \tau, \alpha F$, and increase P , which are interrelated. Therefore, by varying the main parameters ($n, I, \lambda, \tau, \alpha F$) and minimizing their various combinations, it is necessary to conduct a comprehensive comparative assessment of the main characteristics of TEC. Based on the analysis, choose a mode of operation that would reveal which requirements are prevalent, taking into consideration the weight of each of the limiting factors and ease of control.

To calculate the main parameters, reliability indicators, and time of entering the stationary mode of operation for various current modes of operation, the following ratios from [14] are used. The number of thermoelements n of a single-stage TEC can be determined from the following ratio:

$$n = \frac{Q_0}{I_{\max K}^2 R_K (2B_K - B_K^2 - \Theta)}, \quad (1)$$

where Q_0 is the thermal load value, W; $I_{\max K} = (\bar{e}_K T_0)/R_K$ is the maximal working current, A; \bar{e}_K is the average value of the thermoEMF coefficient of the thermoelement branch, at the end of the cooling process, B/K; $R_K = l/(\bar{\sigma}_K S)$ is the electrical resistance of thermoelement branch, Ohm; l and S are, respectively, the height and cross-sectional area of the branch of a thermoelement; $\bar{\sigma}_K$ is the average value of electrical conductivity of a thermoelement branch, S/cm, at the end of the cooling process; T_K is the heat-absorbing junction temperature, K; $B_K = I/I_{\max K}$ is the relative operating current at the end of the cooling process; I is the working current value, A; $\Theta = \Delta T/\Delta T_{\max} = (T - T_0)/\Delta T_{\max}$ is the relative temperature difference; T is the heat-generating junction temperature K; $\Delta T_{\max} = 0.5 \bar{z} T_0^2$ is the maximal temperature difference, K; \bar{z} is the average value of efficiency of initial thermoelectric materials in the module, 1/K.

The power consumption W_K by TEC can be determined from the following expression:

$$W_K = 2n \cdot I_{\max K}^2 \cdot R_K \cdot B_K \left(B_K + \frac{\Delta T_{\max}}{T_0} \Theta \right). \quad (2)$$

Voltage drop U_K :

$$U_K = \frac{W_K}{I}. \quad (3)$$

The refrigeration coefficient E can be calculated:

$$E = \frac{Q_0}{W_K}. \tag{4}$$

The relative value of the failure rate λ/λ_0 can be determined from the following expression given in [14]:

$$\lambda / \lambda_0 = nB_K^2 (\Theta + C) \frac{\left(B_K + \frac{\Delta T_{\max} \Theta}{T_0} \right)^2}{\left(1 + \frac{\Delta T_{\max} \Theta}{T_0} \right)^2} \cdot K_T, \tag{5}$$

where $C = Q_0 / (nI_{\max K}^2 R_K)$ is the relative heat load; K_T is the significant coefficient of low temperatures.

The probability of TEC trouble-free operation P can be determined from the following expression:

$$P = \exp[-\lambda t], \tag{6}$$

where t is the assigned resource, hour.

The ratio for determining the time of entering the stationary mode of operation τ takes the following form given in [15]:

$$\tau = \frac{m_0 C_0 + n \sum_i m_i C_i}{nK \left(1 + 2B_K \frac{\Delta T_{\max}}{T_0} \right)} \ln \frac{\gamma B_H (2 - B_H)}{2B_K - B_K^2 - \Theta}, \tag{7}$$

where $\gamma = (I_{\max H}^2 R_H) / (I_{\max K}^2 R_K)$, $m_0 C_0$ is the product of the mass and heat capacity of the cooled object; $m_0 C_0 \rightarrow 0$ in the absence of a cooled object; $\sum_i m_i C_i$ is the total value of the product of heat capacity and mass of конструктивных и технологических элементов (КТЭ) components on the heat-absorbing module junction at predefined l/S ; $R_H = l / (\sigma_H \cdot S)$ is the electrical resistance of a thermoelement branch at the beginning of the cooling process, Ohm; σ_H is the average value of the electrical conductivity of a thermoelement branch, S/cm, at the beginning of the cooling process; $B_H = I / I_{\max H}$ is the relative operating current at the beginning of the cooling process, at $\tau=0$; $I_{\max H} = (\bar{e}_H \cdot T) / R_H$ is the maximum operating current at the beginning of the cooling process, A.

Provided that the currents are equal at the beginning and end of the cooling process:

$$I = B_K I_{\max K} = B_H I_{\max H}. \tag{8}$$

Based on the results of the research on minimizing the sets of the main parameters in conjunction with the reliability indicators and dynamics of functioning, a series of current operating modes have been developed [12].

Fig. 1, positions 4–7 represent the dependences of the relative operating current $B=f(\Theta)$ on the relative temperature difference Θ for the developed current modes of operation (4) to (7).

Consider several additional current modes of operation of the cooling thermoelement to ensure the completeness of the comparative analysis of functioning for different geometry of the branches of thermoelements (l/S ratio):

a) Mode $(n^2 I)_{\min}$:

$$(n^2 I) = \frac{Q_0^2 I_{\max} B}{I_{\max}^4 R^2 (2B - B^2 - \Theta)^2}, \tag{9}$$

then

$$K = \frac{n^2 I \cdot I_{\max}^3 R^2}{Q_0^2} = \frac{B}{(2B - B^2 - \Theta)^2}. \tag{10}$$

We obtain from the condition $dK/dB=0$:

$$B_{opt} = \frac{1 + \sqrt{1 + 3\Theta}}{3}. \tag{11}$$

The dependence of the optimal relative operating current B_{opt} , corresponding to the minimum of the set on the relative temperature difference Θ , is presented in Fig. 1, position 2.

b) Mode $(n\alpha F)_{\min}$. Using ratio (1) and the expression to determine the heat sink capacity of the radiator:

$$\alpha F = \frac{Q_0 + W}{\Delta T_{\max} (\Theta - \Theta_c)} = \frac{Q_0 (1 + 1/E)}{\Delta T_{\max} (\Theta - \Theta_c)}, \tag{12}$$

where

$$\Theta_{env} = \frac{T_{env} - T_0}{\Delta T_{\max}},$$

T_{env} is the medium temperature, K,

$$1 + 1/E = \frac{2B \left(1 + \frac{\Delta T}{T_0} \Theta \right) + B^2 - \Theta}{2B - B^2 - \Theta},$$

then expression (12) can be written as:

$$\alpha F = \frac{Q_0 \left[2B \left(1 + \frac{\Delta T_{\max} \Theta}{T_0} \right) + B^2 - \Theta \right]}{\Delta T_{\max} (\Theta - \Theta_L) (2B - B^2 - \Theta)}, \tag{13}$$

then the $n\alpha F$ set can be represented as:

$$K = \frac{n\alpha F \cdot I_{\min}^3 R \Delta T_{\max} (\Theta - \Theta_c)}{Q_0^2} = \frac{2B \left(1 + \frac{\Delta T}{T_0} \Theta \right) + B^2 - \Theta}{(2B - B^2 - \Theta)}. \tag{14}$$

We obtain from the condition $dK/dB=0$:

$$B_{opt}^3 + 3B_{opt}^2 \left(1 + \frac{\Delta T_{\max} \Theta}{T_0} \right) - B_{opt} \left[\Theta \left(3 + \frac{2\Delta T_{\max}}{T_0} \right) + 2 \right] + \Theta \left(1 - \frac{\Delta T_{\max}}{T_0} \Theta \right) = 0, \tag{15}$$

The dependence of the optimal relative operating current B_{opt} , corresponding to the minimum of the set $(n\alpha F)_{\min}$, on the relative temperature difference Θ , is presented in Fig. 1, position 3.

c) Mode $Q_0=0$. Using ratio (1), one can write:

$$K = \frac{Q_0}{nI_{\max}^2 R} = 2B - B^2 - \Theta,$$

we obtain at $K \rightarrow 0$

$$B_{opt} = 1 - \sqrt{1 - \Theta}. \tag{16}$$

The dependence of the optimal relative operating current B_{opt} , corresponding to the mode $Q_0=0$, on the relative temperature difference Θ , is presented in Fig. 1, position 9.

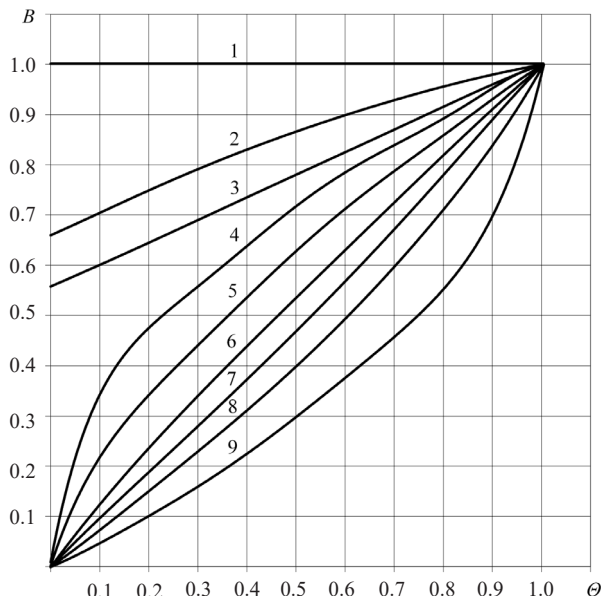


Fig. 1. Dependence of the relative operating current B of a single-stage thermoelectric cooler on the relative temperature difference Θ at $T=300$ K, for different current modes of operation: 1 – mode Q_{0max} ; 2 – mode $(n^2I)_{min}$; 3 – mode $(n\alpha F)_{min}$; 4 – mode $(nI)_{min}$; 5 – mode $(nI\alpha F)_{min}$; 6 – mode $(nI\lambda/\lambda_0\tau)_{min}$; 7 – mode $(nI\lambda/\lambda_0)_{min}$; 8 – mode λ_{min} ; 9 – mode $Q_0=0$

5. 2. Analysis of the thermoelectric cooler model relative to the set of basic parameters

The results of calculations of the main parameters, reliability indicators, time of entering the stationary mode of operation for various current modes of operation

are given in Table 1. The data were obtained at a temperature difference $\Delta T=40$ K, the value of the thermal load $Q_0=0.5$ W, $T=300$ K, $T-T_{env}=5$ K for different geometry of the branches of thermoelements (I/S ratio) $I/S=4.5; 10; 20; 40$.

Table 1

Results of calculations of the main parameters, reliability indicators, time of entering the stationary mode of operation

I/S	Mode of operation	B	$R \cdot 10^3, \text{ Ohm}$	$I_{max}, \text{ A}$	$n, \text{ pcs.}$	$W, \text{ W}$	$U, \text{ V}$	E	$I, \text{ A}$	$\alpha F, \text{ W/h}$	$\tau, \text{ s}$	$N, \text{ W}\cdot\text{s}$	λ/λ_0	$\lambda \cdot 10^8, 1/\text{h}$	P
1	2	3	4	5	6	7	8	9	10	11	12	13	14	15	16
4.5	Q_{0max}	1.0	4.55	11.1	1.8	2.3	0.21	0.216	11.1	0.56	7.8	17.9	1.6	4.8	0.99952
	$(n^2I)_{min}$	0.86			1.9	1.82	0.19	0.275	9.6	0.46	8.0	14.6	1.06	3.2	0.99968
	$(n\alpha F)_{min}$	0.77			2.0	1.60	0.187	0.312	8.55	0.42	8.6	13.7	0.74	2.21	0.99978
	$(nI)_{min}$	0.71			2.3	1.5	0.19	0.34	8.0	0.39	9.2	13.4	0.44	1.53	0.99985
	$(nI\alpha F)_{min}$	0.62			2.5	1.4	0.20	0.37	6.9	0.37	10.2	14.0	0.39	1.2	0.99988
	$(nI\lambda/\lambda_0\tau)_{min}$	0.53			3.2	1.3	0.22	0.38	5.9	0.36	11.9	15.5	0.26	0.77	0.999923
	$(nI\lambda/\lambda_0)_{min}$	0.47			4.1	1.35	0.26	0.37	5.2	0.37	13.9	18.8	0.19	0.58	0.999940
	λ_{min}	0.40			6.6	1.62	0.34	0.31	4.8	0.41	16.0	25.9	0.15	0.46	0.999950
10	Q_{0max}	1.0	10.1	5.02	3.9	2.3	0.46	0.216	5.02	0.56	6.4	14.7	4.0	12.0	0.99880
	$(n^2I)_{min}$	0.86			4.1	1.82	0.42	0.275	4.32	0.46	6.9	12.6	2.35	7.0	0.99930
	$(n\alpha F)_{min}$	0.77			4.4	1.60	0.41	0.313	3.9	0.42	7.4	11.8	1.62	4.9	0.99951
	$(nI)_{min}$	0.71			4.7	1.50	0.41	0.34	3.6	0.39	7.7	11.2	1.23	3.7	0.99963
	$(nI\alpha F)_{min}$	0.62			5.5	1.40	0.44	0.37	3.1	0.37	8.8	12.0	0.85	2.5	0.99975
	$(nI\lambda/\lambda_0\tau)_{min}$	0.53			7.0	1.30	0.49	0.38	2.7	0.36	10.2	13.3	0.56	1.7	0.99983
	$(nI\lambda/\lambda_0)_{min}$	0.47			9.0	1.35	0.57	0.37	2.4	0.37	12.0	16.0	0.42	1.3	0.99987
	λ_{min}	0.40			12.0	1.62	0.81	0.31	2.0	0.41	14.0	22.7	0.36	1.1	0.99990
20	Q_{0max}	1.0	20.2	2.51	7.9	2.3	0.92	0.216	2.51	0.56	6.0	13.9	6.2	18.5	0.9982
	$(n^2I)_{min}$	0.86			8.2	1.82	0.84	0.275	2.16	0.46	6.8	12.3	4.7	14.0	0.9986
	$(n\alpha F)_{min}$	0.77			8.8	1.60	0.83	0.313	1.93	0.42	7.2	11.5	3.2	9.7	0.99903
	$(nI)_{min}$	0.71			10.3	1.50	0.81	0.34	1.80	0.39	7.4	10.8	2.0	6.0	0.99940
	$(nI\alpha F)_{min}$	0.62			11.0	1.40	0.88	0.37	1.56	0.37	8.9	12.1	1.7	5.1	0.99949
	$(nI\lambda/\lambda_0\tau)_{min}$	0.53			14.0	1.30	0.97	0.38	1.34	0.36	10.0	13.0	1.12	3.35	0.99967
	$(nI\lambda/\lambda_0)_{min}$	0.47			17.9	1.35	1.18	0.37	1.18	0.37	11.7	15.6	0.85	2.53	0.99975
	λ_{min}	0.40			29.3	1.62	1.61	0.31	1.0	0.41	13.3	21.5	0.67	2.0	0.99980

Continuation of Table 1

1	2	3	4	5	6	7	8	9	10	11	12	13	14	15	16
40	Q_{0max}	1.0	40.4	1.255	16.0	2.3	1.84	0.216	1.25	0.56	5.2	12.0	12.2	36.7	0.9963
	$(n^2I)_{min}$	0.86			16.4	1.82	1.70	0.275	1.08	0.46	6.0	10.9	9.4	28.1	0.9972
	$(n\alpha F)_{min}$	0.77			17.6	1.60	1.66	0.313	0.97	0.42	6.4	10.2	6.5	19.4	0.9981
	$(nI)_{min}$	0.71			20.8	1.50	1.62	0.34	0.90	0.39	6.8	9.2	4.0	12.0	0.9985
	$(n\alpha F)_{min}$	0.62			22.3	1.40	1.76	0.37	0.80	0.37	7.6	10.4	3.4	10.2	0.9990
	$(nI\lambda/\lambda_0\tau)_{min}$	0.53			28.0	1.30	1.94	0.38	0.67	0.36	8.4	10.9	2.24	6.7	0.9993
	$(nI\lambda/\lambda_0)_{min}$	0.47			35.9	1.34	2.3	0.37	0.59	0.37	9.5	12.7	1.7	5.1	0.99950
	λ_{min}	0.40			59.6	1.62	3.1	0.31	0.53	0.41	11.2	18.1	1.34	4.0	0.99960

With an increase in the relative operating current B at $T=300$ K and a thermal load of $Q_0=0.5$ W and a temperature difference $\Delta T=40$ K for different geometry of the branches of thermoelements (l/S ratio):

– the number of thermoelements n decreases (Fig. 2). The growth of the l/S ratio increases the number of thermoelements n at a predefined relative operating current B . The minimum number of thermoelements n_{min} is provided under the Q_{0max} mode;

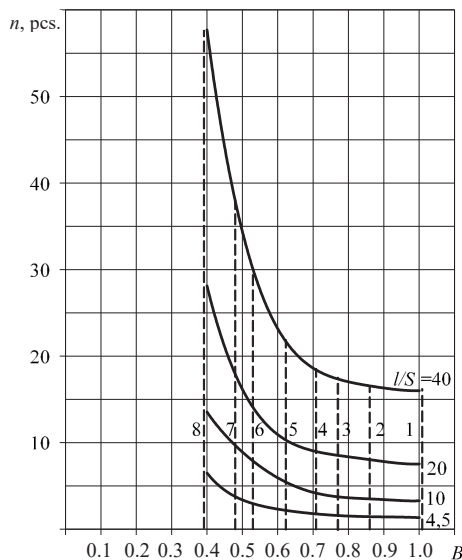


Fig. 2. Dependence of the number of thermoelements n in a single-stage thermoelectric cooler on the relative operating current B for different geometry of thermoelement branches (l/S ratio) at $T=300$ K, $Q_0=0.5$ W, $\Delta T=40$ K: 1 – mode Q_{0max} ; 2 – mode $(n^2I)_{min}$; 3 – mode $(n\alpha F)_{min}$; 4 – mode $(nI)_{min}$; 5 – mode $(n\alpha F)_{min}$; 6 – mode $(nI\lambda/\lambda_0\tau)_{min}$; 7 – mode $(nI\lambda/\lambda_0)_{min}$; 8 – mode λ_{min}

– the functional dependence of the refrigeration coefficient $E=f(B)$ has a maximum at $B=0.53$ under the $(nI\lambda/\lambda_0\tau)_{min}$ mode (Fig. 3). The refrigeration coefficient E does not depend on the geometry of the branches of the thermoelements (l/S ratio). The minimum refrigeration coefficient E_{min} is provided under the $(nI\lambda/\lambda_0\tau)_{min}$ mode;

– the value of working current I increases (Fig. 4). At a predefined value of the relative operating current B , with an increase in the l/S ratio, the value of the operating current I decreases. The maximum operating current is provided under the Q_{0max} mode, and the minimum – under the λ_{min} mode;

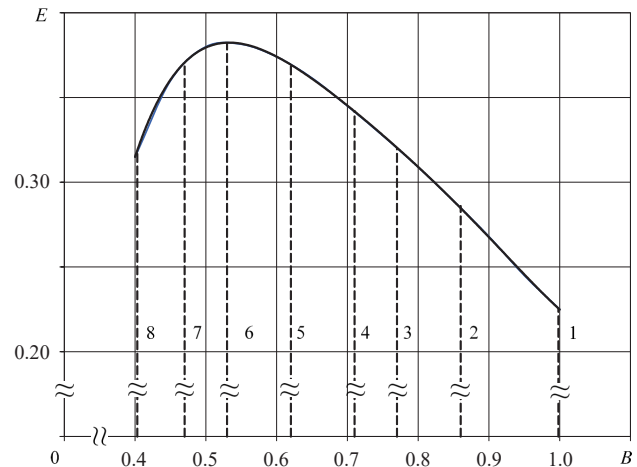


Fig. 3. Dependence of the refrigeration coefficient E of a single-stage thermoelectric cooler on the relative operating current B for different current operating modes at $T=300$ K, $Q_0=0.5$ W, $\Delta T=40$ K: 1 – mode Q_{0max} ; 2 – mode $(n^2I)_{min}$; 3 – mode $(n\alpha F)_{min}$; 4 – mode $(nI)_{min}$; 5 – mode $(n\alpha F)_{min}$; 6 – mode $(nI\lambda/\lambda_0\tau)_{min}$; 7 – mode $(nI\lambda/\lambda_0)_{min}$; 8 – mode λ_{min}

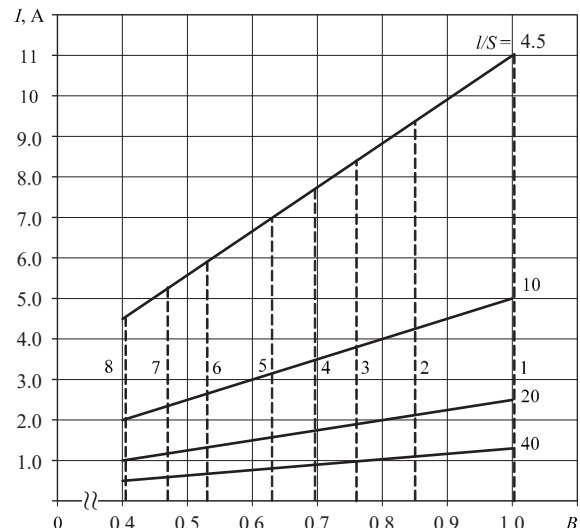


Fig. 4. Dependence of the value of the operating current I of a single-stage thermoelectric cooler on the relative operating current B for different geometry of the branches of thermoelements (l/S ratio) at $T=300$ K, $Q_0=0.5$ W, $\Delta T=40$ K: 1 – mode Q_{0max} ; 2 – mode $(n^2I)_{min}$; 3 – mode $(n\alpha F)_{min}$; 4 – mode $(nI)_{min}$; 5 – mode $(n\alpha F)_{min}$; 6 – mode $(nI\lambda/\lambda_0\tau)_{min}$; 7 – mode $(nI\lambda/\lambda_0)_{min}$; 8 – mode λ_{min}

– the functional dependence of the voltage drop $U=f(B)$ has a minimum at $B=0.71$ under the $(nI)_{\min}$ mode (Fig. 5). With the increase in the l/S ratio, the value of the voltage drop U increases at a predefined relative operating current B . Maximum voltage drops U_{\max} are provided under the λ_{\min} mode;

– the functional dependence $\alpha F=f(B)$ has a minimum at $B=0.53$ under the $(nI\lambda/\lambda_0\tau)_{\min}$ mode (Fig. 6). The heat sink capacity of the radiator αF does not depend on the geometry of the branches of the thermoelements (l/S ratio);

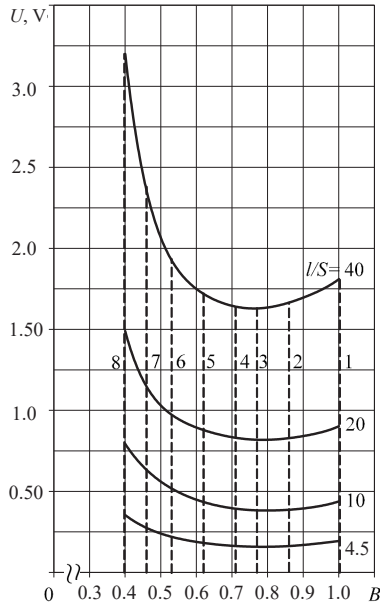


Fig. 5. Dependence of voltage drop U of a single-stage thermoelectric cooler on the relative operating current B for different geometry of thermoelement branches (l/S ratio) at $T=300$ K, $Q_0=0.5$ W, $\Delta T_0=40$ K: 1 – mode $Q_{0\max}$; 2 – mode $(n^2I)_{\min}$; 3 – mode $(n\alpha F)_{\min}$; 4 – mode $(nI)_{\min}$; 5 – mode $(n\alpha F)_{\min}$; 6 – mode $(nI\lambda/\lambda_0\tau)_{\min}$; 7 – mode $(nI\lambda/\lambda_0)_{\min}$; 8 – mode λ_{\min}

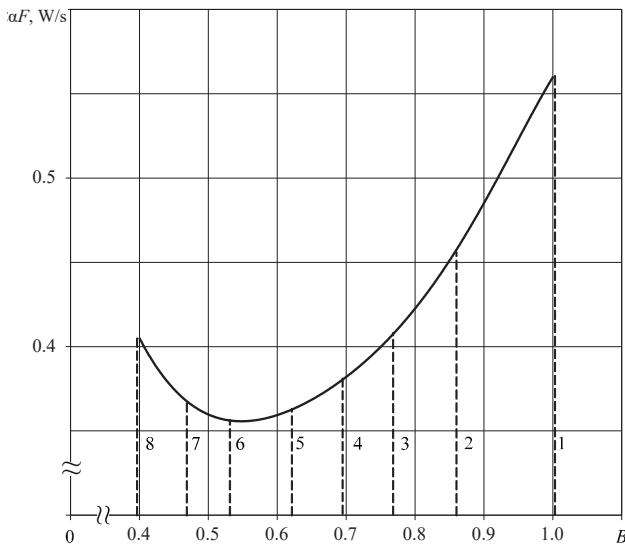


Fig. 6. Dependence of the heat sink capacity of the radiator αF of a single-stage thermoelectric cooler on the relative operating current B at $T=300$ K, $Q_0=0.5$ W, $\Delta T=40$ K, $T-T_{env}=5$ K: 1 – mode $Q_{0\max}$; 2 – mode $(n^2I)_{\min}$; 3 – mode $(n\alpha F)_{\min}$; 4 – mode $(nI)_{\min}$; 5 – mode $(n\alpha F)_{\min}$; 6 – mode $(nI\lambda/\lambda_0\tau)_{\min}$; 7 – mode $(nI\lambda/\lambda_0)_{\min}$; 8 – mode λ_{\min}

– the relative value of the failure rate λ/λ_0 increases (Fig. 7). With the increase in the l/S ratio, the relative value of the failure intensity λ/λ_0 increases at a predefined relative operating current B .

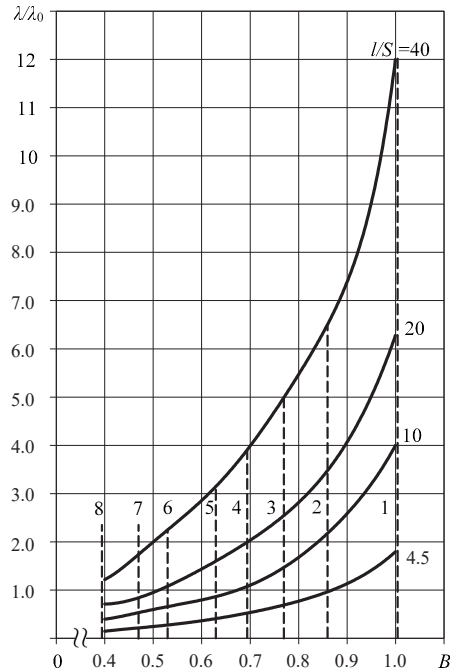


Fig. 7. Dependence of the relative value of the failure rate λ/λ_0 of a single-stage thermoelectric cooler on the relative operating current B for different geometry of the branches of thermoelements (l/S ratio) at $T=300$ K, $Q_0=0.5$ W, $\Delta T=40$ K: 1 – mode $Q_{0\max}$; 2 – mode $(n^2I)_{\min}$; 3 – mode $(n\alpha F)_{\min}$; 4 – mode $(nI)_{\min}$; 5 – mode $(n\alpha F)_{\min}$; 6 – mode $(nI\lambda/\lambda_0\tau)_{\min}$; 7 – mode $(nI\lambda/\lambda_0)_{\min}$; 8 – mode λ_{\min}

The minimum relative failure rate $\lambda/\lambda_{0\min}$ is provided under the λ_{\min} mode. The maximum relative intensity λ/λ_0 is provided under the mode $Q_{0\max}$:

– the probability of trouble-free operation P is reduced (Fig. 8). As the l/S ratio increases, the probability of trouble-free operation P decreases at predefined B . The maximum probability of trouble-free operation P_{\max} is provided under the mode λ_{\min} . The minimum probability of trouble-free operation P is provided under the mode $Q_{0\max}$;

– the time of entering the stationary mode of operation τ is reduced (Fig. 9). With the growth of the l/S ratio, the time of entering the stationary mode of operation τ decreases. The minimum time for entering the stationary mode of operation τ_{\min} is provided under the mode $Q_{0\max}$;

– the functional dependence of the amount of energy expended $N=f(B)$ has a minimum at $B=0.71$ under the mode $(nI)_{\min}$. With an increase in the ratio (l/S), the amount of energy spent N decreases (Fig. 10) at a fixed relative operating current B . The maximum amount of energy spent N_{\max} corresponds to the λ_{\min} mode.

The results of calculations of the main parameters, reliability indicators, time of entering the stationary mode of operation for various current modes of operation of a single-stage TEC at temperature drops from $\Delta T=10$ K to $\Delta T=60$ K, thermal load $Q_0=0.5$ W, $T-T_c=5$ K, $l/S=4.5$ K are given in Table 2.

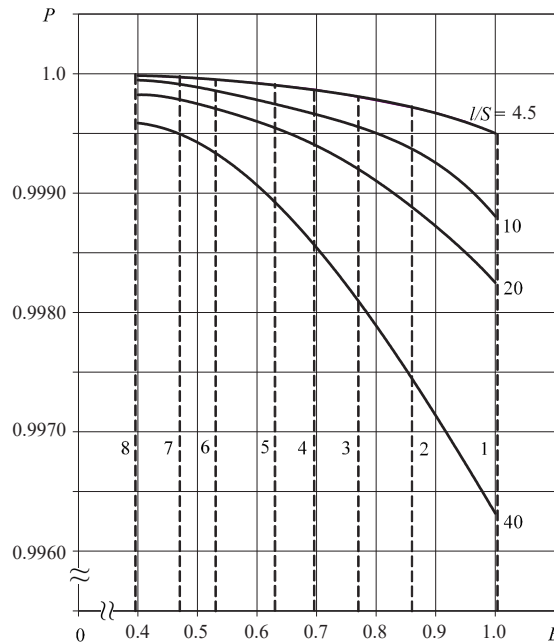


Fig. 8. Dependence of the probability of trouble-free operation P of a single-stage thermoelectric cooler on the relative operating current B for different geometry of thermoelement branches (l/S ratio) at $T=300$ K, $Q_0=0.5$ W, $\Delta T=40$ K: 1 – mode Q_{0max} ; 2 – mode $(n^2I)_{min}$; 3 – mode $(n\alpha F)_{min}$; 4 – mode $(nI)_{min}$; 5 – mode $(n/\alpha F)_{min}$; 6 – mode $(nI/\lambda_0\tau)_{min}$; 7 – mode $(nI/\lambda_0)_{min}$; 8 – mode λ_{min}

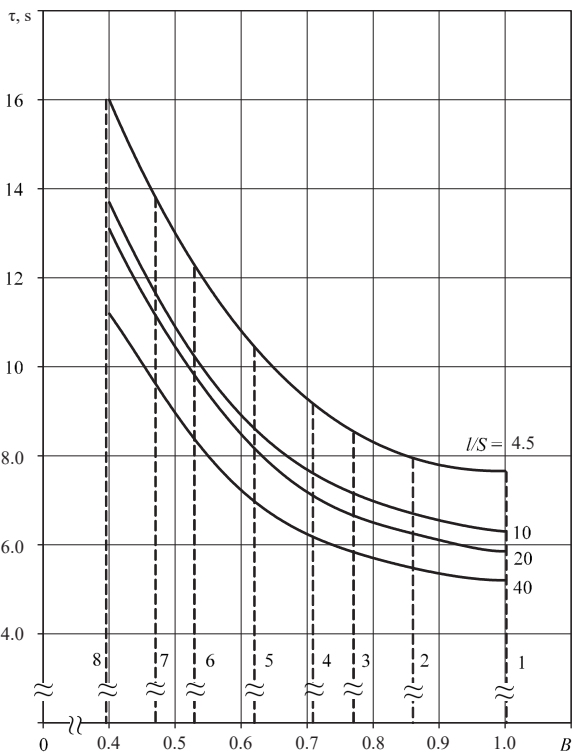


Fig. 9. Dependence of the time of entering the stationary mode of operation τ of a single-stage thermoelectric cooler on the relative operating current B for different geometry of the branches of thermoelements (l/S ratio) at $T=300$ K, $Q_0=0.5$ W, $\Delta T=40$ K: 1 – mode Q_{0max} ; 2 – mode $(n^2I)_{min}$; 3 – mode $(n\alpha F)_{min}$; 4 – mode $(nI)_{min}$; 5 – mode $(n/\alpha F)_{min}$; 6 – mode $(nI/\lambda_0\tau)_{min}$; 7 – mode $(nI/\lambda_0)_{min}$; 8 – mode λ_{min}

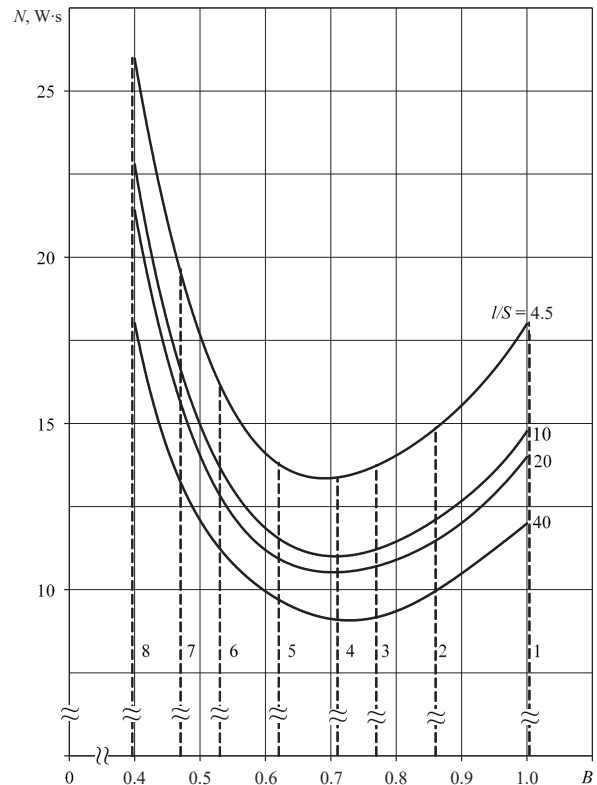


Fig. 10. Dependence of the amount of energy spent N of a single-stage thermoelectric cooler on the relative operating current B for different geometry of the branches of thermoelements (l/S ratio) at $T=300$ K, $Q_0=0.5$ W, $\Delta T=40$ K: 1 – mode Q_{0max} ; 2 – mode $(n^2I)_{min}$; 3 – mode $(n\alpha F)_{min}$; 4 – mode $(nI)_{min}$; 5 – mode $(n/\alpha F)_{min}$; 6 – mode $(nI/\lambda_0\tau)_{min}$; 7 – mode $(nI/\lambda_0)_{min}$; 8 – mode λ_{min}

Table 2

Results of calculations of the main parameters, reliability indicators, time of entering the stationary mode of operation

Mode of operation	B	n, pcs.	W, W	U, V	E	I, A	αF , W/K	B_H	Q_0 , W $n=27$	τ , c	N, W·s	λ/λ_0	$\lambda \cdot 10^8$, 1/h	P
$\Delta T=10$ K, $T_0=290$ K, $\Delta T_{max}=101$ K, $\Theta=0.1$; $R_K=4.89 \cdot 10^{-3}$ Ohm; $I_{maxK}=12.0$ A, $\gamma=1.064$														
Q_{0max}	1.0	0.81	1.13	0.10	0.44	12.0	0.33	0.98	17.0	1.36	1.54	0.80	2.4	0.99976
$(n^2I)_{min}$	0.713	0.87	0.653	0.08	0.766	8.56	0.26	0.70	15.5	1.46	0.95	0.21	0.64	0.999936
$(n\alpha F)_{min}$	0.60	0.96	0.515	0.07	0.97	7.2	0.20	0.59	14.0	1.63	0.84	0.11	0.33	0.999967
$(nI)_{min}$	0.315	1.7	0.25	0.07	1.97	3.8	0.15	0.31	8.14	2.90	0.73	0.01	0.03	0.9999970
$(nI\alpha F)_{min}$	0.215	2.5	0.19	0.073	2.66	2.6	0.14	0.21	5.4	3.8	0.72	0.0026	0.008	0.9999992
$(nI\lambda/\lambda_0\tau)_{min}$	0.113	6.3	0.15	0.11	3.40	1.36	0.13	0.11	2.14	7.9	1.19	0.00035	0.00011	0.99999989
$(nI\lambda/\lambda_0)_{min}$	0.10	7.9	0.15	0.125	3.3	1.20	0.13	0.10	1.7	9.6	1.44	0.00025	0.00077	0.99999924
λ_{min}	0.070	20.7	0.21	0.25	2.4	0.85	0.14	0.072	0.665	16.9	3.55	0.00014	0.00043	0.99999910
$\Delta T=20$ K, $T_0=280$ K, $\Delta T_{max}=93.7$ K; $\Theta=0.213$; $R_K=4.74 \cdot 10^{-3}$ Ohm; $I_{maxK}=11.8$ A, $\gamma=1.135$														
Q_{0max}	1.0	1.0	1.28	0.11	0.39	11.6	0.36	0.96	13.9	3.0	3.8	0.93	2.81	0.99972
$(n^2I)_{min}$	0.76	1.04	0.87	0.10	0.58	8.97	0.27	0.73	12.9	3.15	2.7	0.34	1.03	0.999897
$(n\alpha F)_{min}$	0.65	1.14	0.71	0.092	0.71	7.67	0.24	0.63	11.76	3.47	2.45	0.19	0.58	0.999942
$(nI)_{min}$	0.46	1.6	0.48	0.090	1.04	5.5	0.20	0.45	8.77	4.7	2.26	0.053	0.16	0.999984
$(nI\alpha F)_{min}$	0.35	2.1	0.40	0.10	1.24	4.1	0.18	0.34	6.45	5.7	2.30	0.023	0.070	0.9999930
$(nI\lambda/\lambda_0\tau)_{min}$	0.24	3.7	0.35	0.13	1.41	2.8	0.17	0.23	3.62	8.9	3.16	0.0072	0.0216	0.9999978
$(nI\lambda/\lambda_0)_{min}$	0.20	5.1	0.36	0.15	1.37	2.4	0.172	0.19	2.60	11.3	4.1	0.005	0.0142	0.9999986
λ_{min}	0.16	10.6	0.48	0.27	1.04	1.90	0.20	0.15	1.44	16.5	7.9	0.0032	0.010	0.9999990
$\Delta T=30$ K, $T_0=270$ K, $\Delta T_{max}=86.8$ K; $\Theta=0.346$; $R_K=4.69 \cdot 10^{-3}$ Ohm; $I_{maxK}=11.46$ A, $\gamma=1.22$														
Q_{0max}	1.0	1.30	1.6	0.14	0.32	11.5	0.42	0.94	10.8	4.9	7.74	1.17	3.5	0.99965
$(n^2I)_{min}$	0.81	1.31	1.2	0.13	0.42	9.3	0.34	0.76	10.2	5.2	6.2	0.58	1.74	0.99983
$(n\alpha F)_{min}$	0.71	1.42	1.02	0.125	0.49	8.14	0.30	0.665	9.4	5.6	5.7	0.365	1.1	0.99989
$(nI)_{min}$	0.59	1.76	0.82	0.130	0.61	6.9	0.26	0.55	8.0	6.7	5.5	0.17	0.52	0.999948
$(nI\alpha F)_{min}$	0.48	2.14	0.74	0.135	0.68	5.5	0.25	0.45	6.3	7.9	5.85	0.10	0.31	0.999970
$(nI\lambda/\lambda_0\tau)_{min}$	0.376	3.1	0.70	0.16	0.71	4.3	0.24	0.35	4.36	10.0	7.0	0.052	0.156	0.999984
$(nI\lambda/\lambda_0)_{min}$	0.32	4.2	0.71	0.19	0.70	3.67	0.242	0.30	3.15	12.5	8.9	0.0355	0.107	0.999989
λ_{min}	0.26	7.1	0.87	0.28	0.58	3.2	0.27	0.245	1.75	15.5	13.5	0.027	0.081	0.9999920
$\Delta T=40$ K, $T_0=260$ K, $\Delta T_{max}=79.8$ K; $\Theta=0.50$; $R=4.55 \cdot 10^{-3}$ Ohm; $I_{maxK}=11.11$ A, $\gamma=1.336$														
Q_{0max}	1.0	1.80	2.3	0.21	0.22	11.1	0.56	0.91	7.63	7.8	17.9	1.6	4.8	0.99953
$(n^2I)_{min}$	0.86	1.86	1.82	0.191	0.275	9.55	0.46	0.78	7.33	8.0	14.6	1.06	3.19	0.99968
$(n\alpha F)_{min}$	0.78	1.98	1.615	0.186	0.31	8.66	0.42	0.71	6.90	8.5	13.7	0.766	2.3	0.99977
$(nI)_{min}$	0.71	2.3	1.46	0.19	0.34	8.0	0.39	0.64	6.35	9.2	13.4	0.44	1.53	0.99985
$(nI\alpha F)_{min}$	0.62	2.50	1.37	0.20	0.37	6.9	0.37	0.56	5.43	10.2	14.0	0.39	1.16	0.99988
$(nI\lambda/\lambda_0\tau)_{min}$	0.53	3.2	1.30	0.22	0.38	5.9	0.36	0.48	4.26	11.9	15.5	0.26	0.77	0.999923
$(nI\lambda/\lambda_0)_{min}$	0.47	4.1	1.35	0.26	0.37	5.2	0.37	0.43	3.34	13.9	18.8	0.20	0.58	0.999942
λ_{min}	0.40	6.6	1.62	0.34	0.31	4.8	0.41	0.36	2.14	16.0	25.9	0.155	0.46	0.999954
$\Delta T=50$ K, $T_0=250$ K, $\Delta T_{max}=73.1$ K; $\Theta=0.684$; $R=4.41 \cdot 10^{-3}$ Ohm; $I_{maxK}=10.9$ A, $\gamma=1.43$														
Q_{0max}	1.0	3.1	3.22	0.30	0.155	10.9	0.74	0.89	4.5	12.2	39.3	2.6	7.7	0.99923
$(n^2I)_{min}$	0.915	3.06	3.26	0.33	0.153	10.0	0.75	0.82	4.4	12.3	40.0	2.25	6.74	0.99933
$(n\alpha F)_{min}$	0.86	3.19	3.04	0.32	0.164	9.4	0.71	0.77	4.2	12.7	38.6	1.85	5.55	0.99945
$(nI)_{min}$	0.83	3.7	2.73	0.34	0.18	9.1	0.69	0.74	4.05	13.1	36.0	1.24	3.7	0.99950
$(nI\alpha F)_{min}$	0.77	3.7	2.80	0.34	0.18	8.4	0.67	0.70	3.70	14.0	39.2	1.4	4.2	0.99958
$(nI\lambda/\lambda_0\tau)_{min}$	0.71	4.1	2.77	0.36	0.18	7.7	0.65	0.63	3.27	15.0	41.6	1.12	3.4	0.99966
$(nI\lambda/\lambda_0)_{min}$	0.66	4.8	2.81	0.39	0.178	7.14	0.66	0.58	2.82	16.4	46.1	0.95	2.85	0.99972
λ_{min}	0.58	7.9	3.4	0.57	0.145	6.8	0.79	0.516	1.97	17.9	61.6	0.79	2.37	0.99976
$\Delta T=60$ K, $T_0=240$ K, $\Delta T_{max}=66.8$ K; $\Theta=0.90$; $R=4.33 \cdot 10^{-3}$ Ohm; $I_{maxK}=10.5$ A, $\gamma=1.57$														
Q_{0max}	1.0	10.5	12.55	1.20	0.04	10.5	2.61	0.86	1.30	22.9	287	10.9	32.6	0.99675
$(n^2I)_{min}$	0.975	10.5	12.0	1.18	0.0417	10.2	2.50	0.83	1.29	22.1	265	9.9	29.7	0.9970
$(n\alpha F)_{min}$	0.96	10.6	11.8	1.17	0.0423	10.1	2.46	0.825	1.277	22.2	263	9.5	28.5	0.99715
$(nI)_{min}$	0.95	10.8	11.75	1.18	0.0426	9.97	2.45	0.817	1.270	23.2	273	9.23	27.7	0.9972
$(nI\alpha F)_{min}$	0.93	11.0	11.55	1.18	0.0433	9.77	2.41	0.80	1.23	23.3	269	8.73	26.2	0.9974
$(nI\lambda/\lambda_0\tau)_{min}$	0.91	11.4	11.5	1.20	0.0434	9.56	2.40	0.78	1.19	23.4	269	8.34	25.0	0.9975
$(nI\lambda/\lambda_0)_{min}$	0.89	12.0	11.53	1.24	0.0434	9.30	2.40	0.76	1.14	23.6	272	7.9	23.8	0.9976
λ_{min}	0.84	14.1	12.35	1.4	0.0405	8.80	2.57	0.72	0.97	23.8	294	7.63	22.9	0.99771

With the increase in temperature difference ΔT for different current operating modes at $Q_0=0.5$ W, $I/S=4.5$:

- the relative operating current B (Fig. 11) increases except for the Q_{0max} mode ($B=1$). With a fixed temperature difference ΔT , the relative operating current B increases from the λ_{min} mode to the Q_{0max} mode;

- the functional dependence of the number of thermoelements $n=f(\Delta T)$ has a minimum at $\Delta T=40$ K except for the mode Q_{0max} , $(nI)_{min}$, $(nI\alpha F)_{min}$ (Fig. 12). With a fixed temperature difference ΔT , the number of thermoelements n decreases from the λ_{min} mode to the Q_{0max} mode;

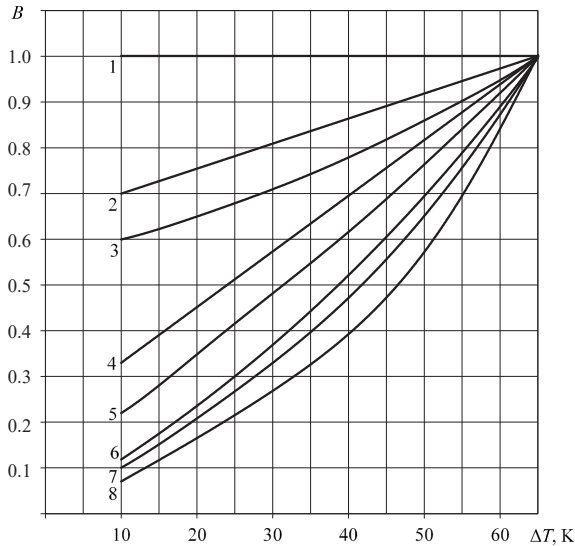


Fig. 11. Dependence of the relative operating current B of the single-stage thermoelectric cooler on the temperature difference ΔT for different current operating modes at $T=300$ K, $I/S=4.5$, $Q_0=0.5$ V: 1 – mode Q_{0max} ; 2 – mode $(n^2I)_{min}$; 3 – mode $(n\alpha F)_{min}$; 4 – mode $(nI)_{min}$; 5 – mode $(nI\alpha F)_{min}$; 6 – mode $(nI\lambda/\lambda_0\tau)_{min}$; 7 – mode $(nI\lambda/\lambda_0)_{min}$; 8 – mode λ_{min}

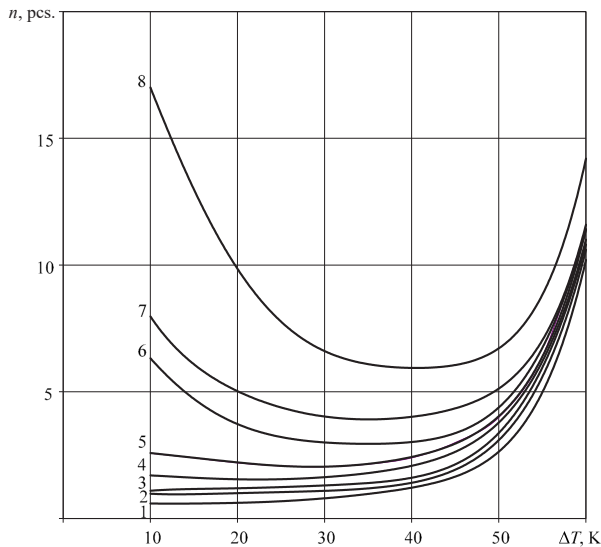


Fig. 12. Dependence of the number of thermoelements n in a single-stage thermoelectric cooler on the temperature difference ΔT for different current modes of operation at $T=300$ K, $Q_0=0.5$ W, $I/S=4.5$: 1 – mode Q_{0max} ; 2 – mode $(n^2I)_{min}$; 3 – mode $(n\alpha F)_{min}$; 4 – mode $(nI)_{min}$; 5 – mode $(nI\alpha F)_{min}$; 6 – mode $(nI\lambda/\lambda_0\tau)_{min}$; 7 – mode $(nI\lambda/\lambda_0)_{min}$; 8 – mode λ_{min}

- the value of the operating current I (Fig. 13) increases except for the Q_{0max} mode. Under the mode Q_{0max} , the value of the operating current I decreases;

- the value of the operating current I decreases from the Q_{0max} mode to the λ_{min} mode;
- the refrigeration coefficient E decreases (Fig. 14).

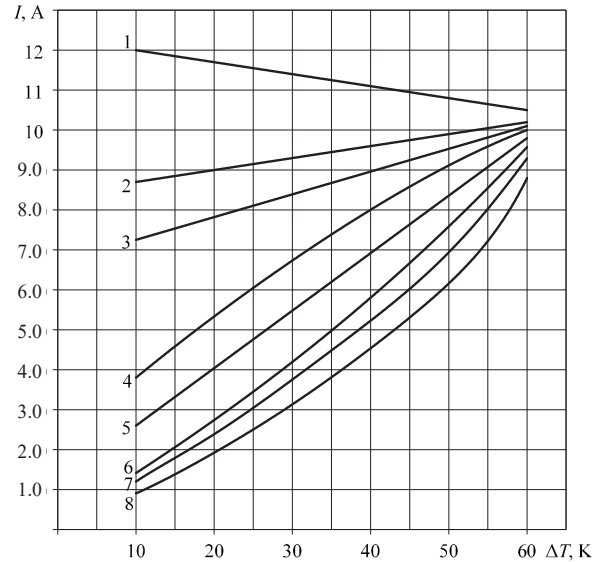


Fig. 13. Dependence of the operating current I of a single-stage thermoelectric cooler on the temperature difference ΔT for different current modes of operation at $T=300$ K, $Q_0=0.5$ W, $I/S=4.5$: 1 – mode Q_{0max} ; 2 – mode $(n^2I)_{min}$; 3 – mode $(n\alpha F)_{min}$; 4 – mode $(nI)_{min}$; 5 – mode $(nI\alpha F)_{min}$; 6 – mode $(nI\lambda/\lambda_0\tau)_{min}$; 7 – mode $(nI\lambda/\lambda_0)_{min}$; 8 – mode λ_{min}

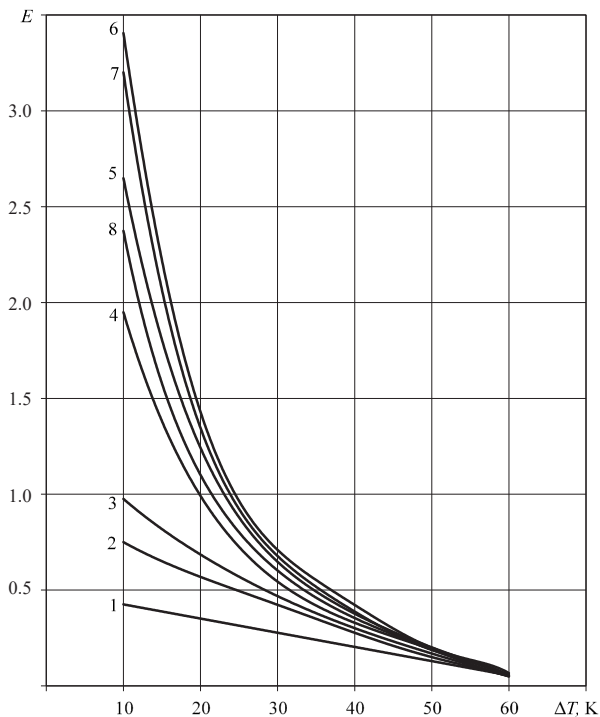


Fig. 14. Dependence of the refrigeration coefficient E of a single-stage thermoelectric cooler on the temperature difference ΔT for different current operating modes at $T=300$ K, $Q_0=0.5$ W: 1 – mode Q_{0max} ; 2 – mode $(n^2I)_{min}$; 3 – mode $(n\alpha F)_{min}$; 4 – mode $(nI)_{min}$; 5 – mode $(nI\alpha F)_{min}$; 6 – mode $(nI\lambda/\lambda_0\tau)_{min}$; 7 – mode $(nI\lambda/\lambda_0)_{min}$; 8 – mode λ_{min}

The maximum refrigeration coefficient E_{max} is provided under the mode $(nI\lambda/\lambda_0\tau)_{min}$:

– the time of entering the stationary mode of operation τ increases (Fig. 15).

The minimum time to enter the stationary mode of operation τ_{min} is provided under the mode Q_{0max} :

– the heat sink capacity of the radiator αF increases (Fig. 16).

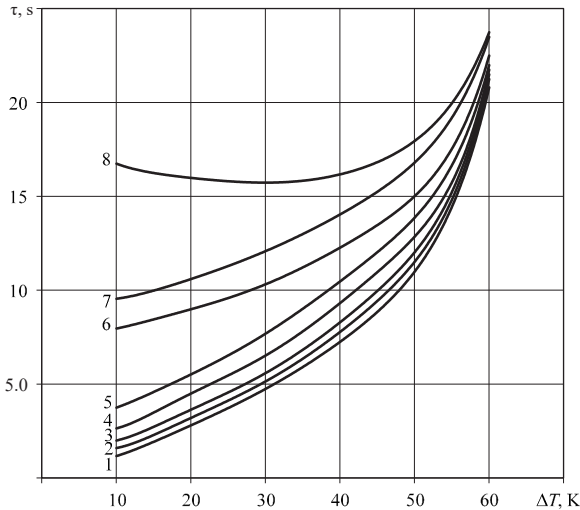


Fig. 15. Dependence of the time of entering the stationary mode of operation τ of a single-stage thermoelectric cooler on the temperature difference ΔT for different current modes of operation at $T=300$ K, $Q_0=0.5$ W, $I/S=4.5$:
 1 – mode Q_{0max} ; 2 – mode $(n^2I)_{min}$; 3 – mode $(n\alpha F)_{min}$;
 4 – mode $(nI)_{min}$; 5 – mode $(n/\alpha F)_{min}$; 6 – mode $(nI\lambda/\lambda_0\tau)_{min}$;
 7 – mode $(nI\lambda/\lambda_0)_{min}$; 8 – mode λ_{min}

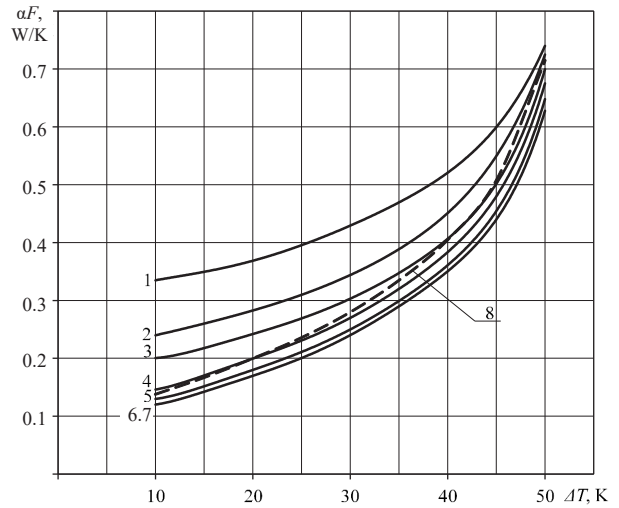


Fig. 16. Dependence of the heat sink capacity of the radiator αF of a single-stage thermoelectric cooler on the temperature difference ΔT for different current modes of operation at $T=300$ K, $Q_0=0.5$ W, $I/S=4.5$: 1 – mode Q_{0max} ;
 2 – mode $(n^2I)_{min}$; 3 – mode $(n\alpha F)_{min}$; 4 – mode $(nI)_{min}$;
 5 – mode $(n/\alpha F)_{min}$; 6 – mode $(nI\lambda/\lambda_0\tau)_{min}$;
 7 – mode $(nI\lambda/\lambda_0)_{min}$; 8 – mode λ_{min}

Minimum heat sink capacity of the radiator αF_{min} is provided under the mode $(nI\lambda/\lambda_0\tau)_{min}$:

– the relative failure rate λ/λ_0 increases (Fig. 17). The minimum value $(\lambda/\lambda_0)_{min}$ is provided under the mode λ_{min} ;

– the probability of trouble-free operation P decreases (Fig. 18). The maximum probability of trouble-free operation P_{max} is provided under the mode λ_{min} ;

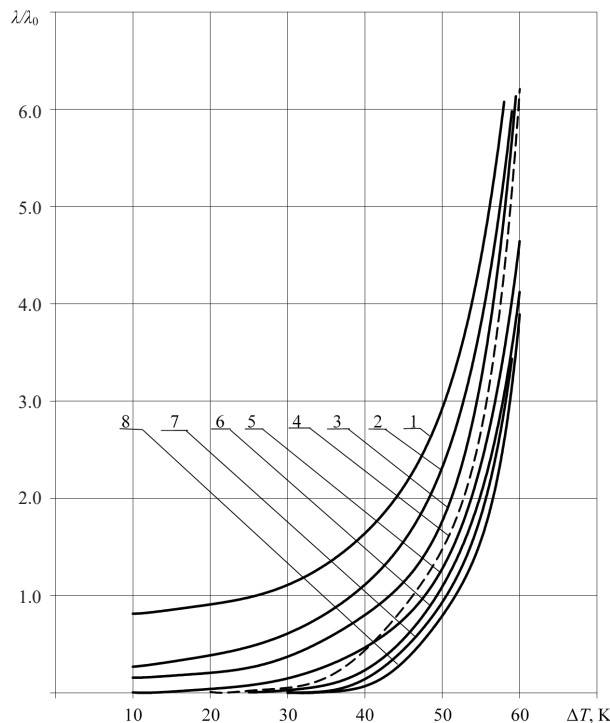


Fig. 17. Dependence of the relative value of the failure intensity λ/λ_0 of a single-stage thermoelectric cooler on the temperature difference ΔT for different current modes of operation at $T=300$ K, $Q_0=0.5$ W, $I/S=4.5$:
 1 – mode Q_{0max} ; 2 – mode $(n^2I)_{min}$; 3 – mode $(n\alpha F)_{min}$; 4 – mode $(nI)_{min}$; 5 – mode $(n/\alpha F)_{min}$;
 6 – mode $(nI\lambda/\lambda_0\tau)_{min}$; 7 – mode $(nI\lambda/\lambda_0)_{min}$; 8 – mode λ_{min}

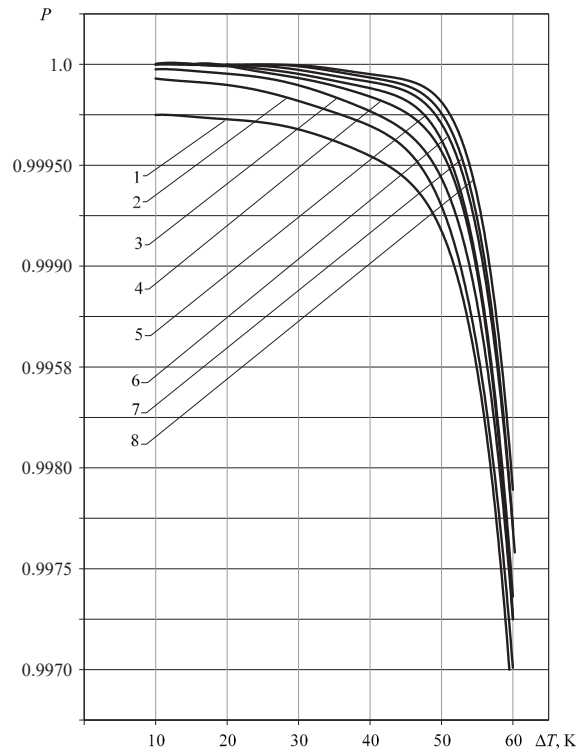


Fig. 18. Dependence of the probability of trouble-free operation P of a single-stage thermoelectric cooler on the temperature difference ΔT for different current modes of operation at $T=300$ K, $Q_0=0.5$ W, $I/S=4.5$: 1 – mode Q_{0max} ; 2 – mode $(n^2I)_{min}$; 3 – mode $(n\alpha F)_{min}$; 4 – mode $(nI)_{min}$; 5 – mode $(n/\alpha F)_{min}$; 6 – mode $(nI/\lambda_0\tau)_{min}$; 7 – mode $(nI/\lambda_0)_{min}$; 8 – mode λ_{min}

– the cooling capacity Q_0 (at $n=27$ pcs) of the single-stage TEC for the operating modes Q_{0max} , $(n^2I)_{min}$, $(n\alpha F)_{min}$ (Fig. 19, positions 1–3) decreases;

– the functional dependence of cooling capacity $Q_0=f(\Theta)$ has a maximum at:

- 1) $\Theta=0.213$ under the mode $(nI)_{min}$ (Fig. 19, position 4);
 - 2) $\Theta=0.28$ under the mode $(n/\alpha F)_{min}$ (Fig. 19, position 5);
 - 3) $\Theta=0.42$ under the mode $(nI/\lambda_0\tau)_{min}$ (Fig. 19, position 6);
 - 4) $\Theta=0.50$ under the mode $(nI/\lambda_0)_{min}$ (Fig. 19, position 7);
 - 5) $\Theta=0.6$ under the mode (λ_{min}) (Fig. 19, position 8);
- the amount of energy expended N increases (Fig. 20).

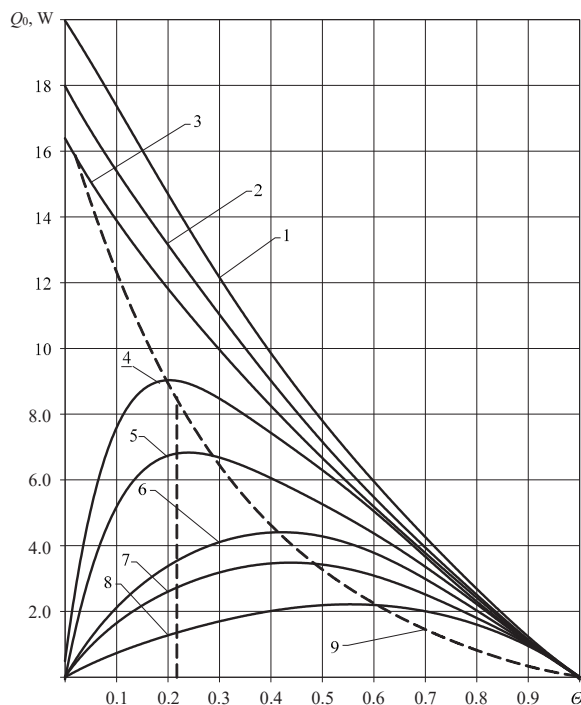


Fig. 19. Dependence of cooling capacity Q_0 of a single-stage thermoelectric cooler on the relative temperature difference Θ for different operating modes at $T=300$ K, $I/S=4.5$, $n=27$ pcs.: 1 – mode Q_{0max} ; 2 – mode $(n^2I)_{min}$; 3 – mode $(n\alpha F)_{min}$; 4 – mode $(nI)_{min}$; 5 – mode $(n/\alpha F)_{min}$; 6 – mode $(nI/\lambda_0\tau)_{min}$; 7 – mode $(nI/\lambda_0)_{min}$; 8 – mode λ_{min} ; 9 – $Q_0=0$

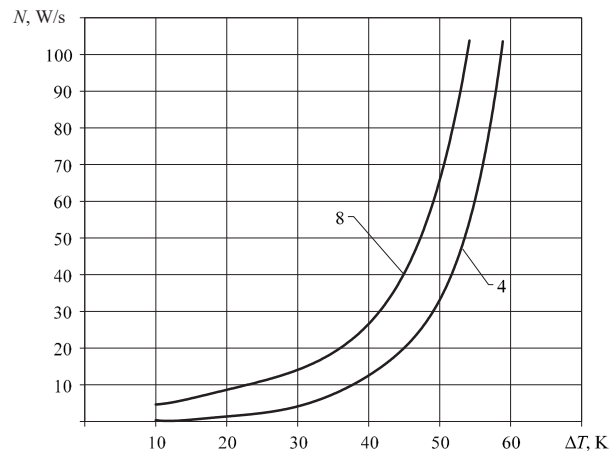


Fig. 20. Dependence of the amount of energy spent N by a single-stage thermoelectric cooler on the temperature difference ΔT for different operating modes at $T=300$ K, $Q_0=0.5$ W, $I/S=4.5$: 4 – mode $(nI)_{min}$; 8 – mode λ_{min}

The minimum amount of energy N_{min} expended is provided under the mode $(nI)_{min}$ (Fig. 20, position 4), and the maximum amount of energy spent N_{max} corresponds to the λ_{min} mode (Fig. 20, position 8).

6. Discussion of results of analyzing the use of basic parameters

Our results are explained, first of all, by the revealed analytical connection between the design parameters of the thermoelectric cooler and the operational indicator of the failure intensity, current operating modes, and the probability of trouble-free operation indicator, entering the steady mode, and the operating temperature difference. Studying analytical functions is much simpler than experimental dependences and makes it possible, already at the design stage, to identify their extreme values (Fig. 6, 10, 13, 19). The nature of changes in the weight and size indicators of the system for ensuring thermal regimes (Fig. 6), the influence of energy indicators on the intensity of failures (Fig. 7), temperature differences on the time of entering the stationary mode (Fig. 15) makes it possible to identify compromise design solutions.

To resolve the issue of ensuring the specified reliability when controlling the cooling capacity of the thermoelectric cooler, a comparative analysis of the main parameters, the indicators of reliability and dynamics of the functioning of a single-stage TEC under various characteristic current modes of operation was carried out. The obtained results showed the possibility of optimal control over the thermal mode of operation by selecting the thermal mode of operation, taking into consideration the weight of each of the limiting factors. A distinctive feature of using a set of basic parameters instead of controlling each of them is to increase the response speed of the system with TEC in the feedback chain and optimize energy indicators. Thus, the minimization of the set in conjunction with the reliability indicators and dynamics of the functioning of the thermoelement provides:

- the maximum refrigeration coefficient E_{\max} and the minimum heat sink capacity of the radiator αF_{\min} under the mode $(nI/\lambda_0\tau)_{\min}$ and does not depend on the geometry of the branches of thermoelements;
- the minimum amount of energy N_{\min} expended and the minimum voltage drop U_{\min} under the mode $(nI)_{\min}$;
- the minimum time of entering the stationary mode of operation τ_{\min} and the minimum number of thermoelements n_{\min} under the mode $Q_{0\max}$;
- the minimum operating current value I_{\min} , the minimum relative failure rate $(\lambda/\lambda_0)_{\min}$, and, therefore, the maximum probability of trouble-free operation P_{\max} and the maximum drop voltage U_{\max} under the mode λ_{\min} .

Our study of operational limitations showed that with an increase in temperature difference ΔT at thermal load $Q_0=0.5$ W and $l/S=4.5$:

- the relative operating current B , the value of the operating current I , the amount of energy spent N , the heat sink capacity of the radiator αF are increased;
- there is an increase in the time of entering the stationary mode of operation τ , the relative failure rate λ/λ_0 ,

and the number of thermoelements n for the modes $Q_{0\max}$, $(n^2I)_{\min}$, $(n\alpha F)_{\min}$;

- there is a decrease in the refrigeration coefficient E , the probability of trouble-free operation P , the cooling capacity Q_0 at a predefined number of thermoelements n under the mode $Q_{0\max}$, $(n^2I)_{\min}$, $(n\alpha F)_{\min}$.

The practical significance of the present research is to optimize control over thermoelectric coolers in the system for providing heat-loaded elements. This is achieved due to the fact that for the operating modes $(nI)_{\min}$, $(nI\alpha F)_{\min}$, $(nI/\lambda_0\tau)_{\min}$, $(nI/\lambda_0)_{\min}$, λ_{\min} the functional dependence $Q_0=f(\Theta)$ has a maximum for different Θ , and the dependence $n=f(\Delta T)$ has a minimum for different ΔT . The devised method of optimal control over the thermal regime of a single-stage TEC based on minimizing the set of basic parameters makes it possible to search for and select compromise solutions, taking into consideration the weight of each limiting factor.

The structural limitations of the use of the proposed model have been analyzed, which showed that with an increase in the l/S ratio at a predefined temperature difference of $\Delta T=40$ K and a thermal load of $Q_0=0.5$ W:

- there is an increase in the number of thermoelements n , voltage drop U , which leads to an increase in the relative failure rate λ/λ_0 ;
- the value of the operating current I decreases, and, as a result, the probability of trouble-free operation P .

Further research could address minimizing the failure rates of the thermoelectric cooler in the operating range of temperature changes and changing operating temperature conditions.

7. Conclusions

1. A mathematical model of the connection of the set of basic parameters with the structural, energy, time, and reliability indicators of a single-stage thermoelectric cooler has been built, which provides a choice of optimized solutions depending on the design goals. A distinctive feature of the model is that the set of parameters includes physically heterogeneous values: structural, energy, operational, temporal, which, in combination, produce a new result – improving the quality of control.

2. The mathematical model was analyzed in the operating range of temperature differences ΔT from 0 to 60 K and the structural parameters of the geometry of thermoelements $l/S=4.5$; 10; 20; 40. Extreme values for the refrigeration coefficient (Fig. 3), energy expended (Fig. 10), heat dissipation capacity of the radiator (Fig. 6), cooling capacity (Fig. 19) have been determined, providing for the possibility of optimal control over the thermal mode of operation. It is shown that the gain in the refrigeration coefficient under the mode $(nI/\lambda_0\tau)_{\min}$, in comparison with the maximum cooling capacity regime, amounts to 1.4 times.

References

1. Shalumova, N. A., Shalumov, A. S., Martynov, O. Yu., Bagayeva, T. A. (2011). Analysis and provision of thermal characteristics of radioelectronic facilities using the subsystem ASONIKA-T. *Advances in modern radio electronics*, 1, 42–49.
2. Sootsman, J. R., Chung, D. Y., Kanatzidis, M. G. (2009). New and Old Concepts in Thermoelectric Materials. *Angewandte Chemie International Edition*, 48 (46), 8616–8639. doi: <https://doi.org/10.1002/anie.200900598>
3. Choi, H.-S., Seo, W.-S., Choi, D.-K. (2011). Prediction of reliability on thermoelectric module through accelerated life test and Physics-of-failure. *Electronic Materials Letters*, 7 (3), 271–275. doi: <https://doi.org/10.1007/s13391-011-0917-x>

4. Eslami, M., Tajeddini, F., Etaati, N. (2018). Thermal analysis and optimization of a system for water harvesting from humid air using thermoelectric coolers. *Energy Conversion and Management*, 174, 417–429. doi: <https://doi.org/10.1016/j.enconman.2018.08.045>
5. Bakhtiaryfard, L., Chen, Y. S. (2014). Design and Analysis of a Thermoelectric Module to Improve the Operational Life. *Advances in Mechanical Engineering*, 7 (1), 152419. doi: <https://doi.org/10.1155/2014/152419>
6. Erturun, U., Mossi, K. (2012). A Feasibility Investigation on Improving Structural Integrity of Thermoelectric Modules With Varying Geometry. Volume 2: Mechanics and Behavior of Active Materials; Integrated System Design and Implementation; Bio-Inspired Materials and Systems; Energy Harvesting. doi: <https://doi.org/10.1115/smasis2012-8247>
7. Manikandan, S., Kaushik, S. C., Yang, R. (2017). Modified pulse operation of thermoelectric coolers for building cooling applications. *Energy Conversion and Management*, 140, 145–156. doi: <https://doi.org/10.1016/j.enconman.2017.03.003>
8. Wang, L. Q., Zhou, L., Fan, H. T. (2013). Design of Cooling System for Infrared CCD Camera Used to Monitor Burden Surface of Blast Furnace Based on Thermoelectric Coolers. *Applied Mechanics and Materials*, 419, 778–783. doi: <https://doi.org/10.4028/www.scientific.net/amm.419.778>
9. Venkatesan, K., Venkataramanan, M. (2020). Experimental and Simulation Studies on Thermoelectric Cooler: A Performance Study Approach. *International Journal of Thermophysics*, 41 (4). doi: <https://doi.org/10.1007/s10765-020-2613-2>
10. Li, H., Ding, X., Meng, F., Jing, D., Xiong, M. (2019). Optimal design and thermal modelling for liquid-cooled heat sink based on multi-objective topology optimization: An experimental and numerical study. *International Journal of Heat and Mass Transfer*, 144, 118638. doi: <https://doi.org/10.1016/j.ijheatmasstransfer.2019.118638>
11. Yu, J., Zhu, Q., Kong, L., Wang, H., Zhu, H. (2020). Modeling of an Integrated Thermoelectric Generation-Cooling System for Thermoelectric Cooler Waste Heat Recovery. *Energies*, 13 (18), 4691. doi: <https://doi.org/10.3390/en13184691>
12. Dong, X., Liu, X. (2019). Multi-objective optimal design of microchannel cooling heat sink using topology optimization method. *Numerical Heat Transfer, Part A: Applications*, 77 (1), 90–104. doi: <https://doi.org/10.1080/10407782.2019.1682872>
13. Irshad, K., Almalawi, A., Khan, A. I., Alam, M. M., Zahir, M. H., Ali, A. (2020). An IoT-Based Thermoelectric Air Management Framework for Smart Building Applications: A Case Study for Tropical Climate. *Sustainability*, 12 (4), 1564. doi: <https://doi.org/10.3390/su12041564>
14. Zaykov, V. P., Kinshova, L. A., Moiseev, V. F. (2009). Prognozirovanie pokazateley nadezhnosti termoelektricheskikh ohlazhdayuschih ustroystv. Kn. 1. Odnokaskadnye ustroystva. Odessa: Politekhpriodika, 120.
15. Zaykov, V. P., Mescheryakov, V. I., Zhuravlev, Yu. I. (2019). Prognozirovanie pokazateley nadezhnosti termoelektricheskikh ohlazhdayuschih ustroystv. Kn. 4. Dinamika funktsionirovaniya odnokaskadnyh TEU. Odessa: Politekhpriodika, 290.